Fluorescence sensors for parallel measurements in multichannel microfluidic devices covering the full channel cross sections

G. Meineke*[a], D. Flitsch[b], A. Lenenbach[a], R. Noll[a]
[a]Fraunhofer Institut for Laser Technology, Steinbachstraße 15, 52074 Aachen, Germany
[b]Chair for Laser Technology LLT, RWTH Aachen University, Steinbachstraße 15, 52074 Aachen, Germany

Sensitive fluorescence sensors are needed to measure single cell properties in microfluidic devices. Optimizing the parallelizability and the measurement volume are two options enabling high throughput applications. The fluorescence sensor presented is highly parallelizable and, due to MEMS micromirror arrays, several sensors can be integrated in one multichannel microfluidic system. The fluorescence sensor has a detection volume of a few thousand femtoliters, covering the full cross-sections of the microfluidic channels used and can be easily adjusted to other cross-section geometries. By measuring labeled particles with diameters below 10 µm we qualified the applicability of the sensor with different channel geometries. The sensors have measurement volumes fitted to the channel geometries with widths from 20 µm up to 400 µm and reach a decision limit of less than 1790 molecules of equivalent soluble fluorophore.

Keywords: µTAS, µFACS, measurement volume, fluorescence, microfluidic devices, single cell analysis

1. INTRODUCTION

In recent years, microfluidic devices have created new possibilities and methods to investigate microbiological research questions on the single cell level. In particular, the possibility to manipulate and analyze single cells opens up the opportunity to discover differences in between cells within seemingly homogeneous cell populations[1]. The major component is often an integrated micro total analysis system (µTAS), which is based on sensors that measure the spectral impedance, light extinction, light scattering or fluorescence emission[2]. Detecting the latter has become a powerful tool because of the high sensitivity and versatility of available fluorescence staining methods, which enable microbiologists to stain microbial cells according to their individual biochemical, physiological or taxonomic properties[3]. Several papers were published concerning the use of fluorescence sensors in microfluidics[4-9]. Increasing sensitivity of the sensors is achieved by reducing measurement volumes using a confocal set-up[5,6], hydrodynamic focusing[8,10] and polarization filtering[9]. For high throughput applications, parallelization is a promising solution involving multiple probing locations. One shown solution uses a fast scanning confocal sensor[10].

We pursue two methods to increase higher throughput in microfluidic systems. On the one hand, we reduce the size of the optical components and implement a multichannel detector. This enables to setup identical sensors with pitches of less than 6 mm on the same chip, making parallelization possible. On the other hand, we use chosen measurement volumes covering the full cross-section of the channel with no need of hydrodynamic focusing, allowing for high flow rates at reduced pressure drops and flow velocities. The drawback of this approach is the decrease of sensitivity, because of the low numerical apertures used and the auto fluorescence signal recorded from the solvent, present in the huge measurement volume.

2. EXPERIMENTAL SET UP

2.1 Sensor assembly

The setup with two independent measurement channels is shown in Fig. 1. The light source used is an Ar-ion laser at a wavelength of 488 nm coupled to a single mode fiber. Two fiber collimators are used to collimate the excitation light. A dichroic beamsplitter with a cutoff wavelength of 500 nm directs the light towards lenses with a diameter of 5 mm and focal lengths of 6.2 mm to focus the laserbeam and to collect the fluorescence light. The collected fluorescence light passes the dichroic mirror and is detected by a multianode photomultiplier (H7546B-20, Hamamatsu). One filter for the excitation light passes light within the wavelength interval between 486 nm and 490 nm and another filter for the fluorescence light between 566 nm and 590 nm. The possibility to insert MEMS micro mirrors between the dichroic and

*georg.meineke@ilt.fraunhofer.de phone + 49 241 8906 - 489; fax + 49 241 8906 - 121; www.ilt.fraunhofer.de

the focusing lenses allows to direct the light beams independently to focusing lenses, which could be placed above a microfluidic device according to the respective microchannel structure.

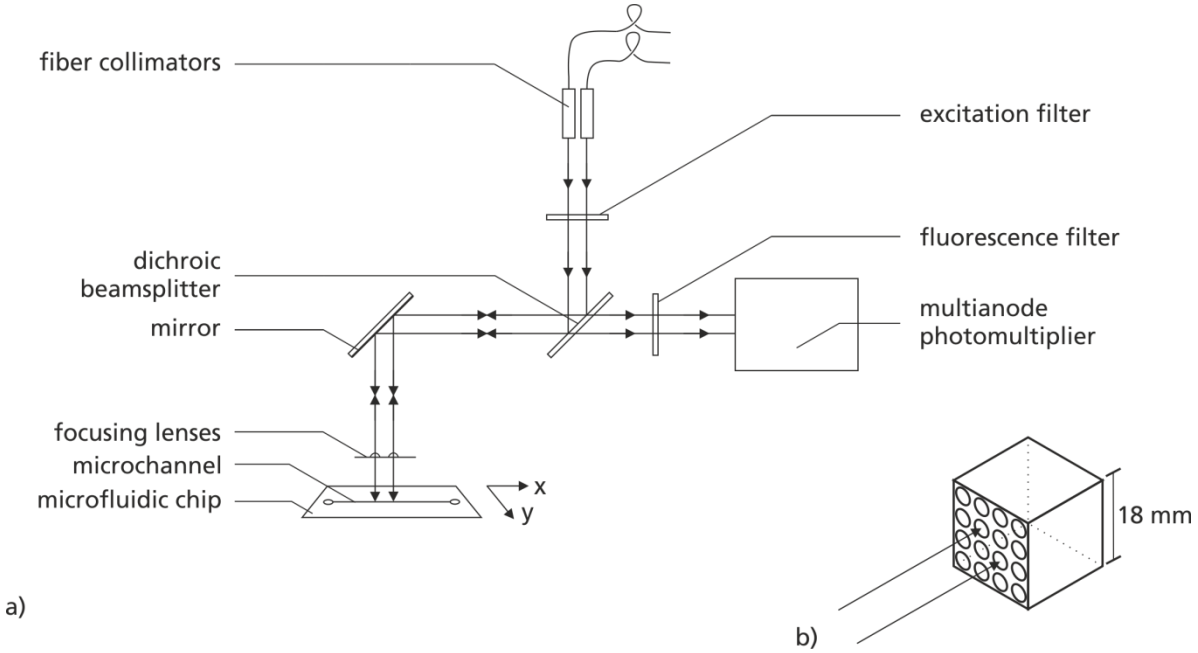

Fig. 1. Setup of parallel fluorescence sensors. a) Optical beam paths and microfluidic chip with two independent measurement channels. b) 3D view of multianode photomultiplier configuration.

2.2 Materials and Methods

Micro beads labeled with the fluorophore phycoerythrin (PE) are used to characterize the parallel sensors. These micro beads (Quantibrite PE Beads, BD Biosciences) are delivered in populations conjugated with different levels of PE. The conjugation level is quantified by the manufacturer and given as molecules of equivalent soluble fluorophore (MESF)[11].

The measurement volume is determined with a fluorophore stained bead immobilized on a glass slide. The sensor records a 2D map of the relative sensitivity while a motorized microscope stage moves the slide laterally through the measurement volume. When the slide is displaced vertically, the measurement volume is finally characterized in 3D.

A microfluidic channel is used to determine decision and detection limits[12]. The channel is 25 µm wide and embedded with a depth of 150 µm in a 200 µm thick silicon wafer and covered by borofloat glass having a thickness of 500 µm. A suspension of micro beads is prepared with three MESF PE levels of 5359, 23843 and 62336 in phosphate buffered saline with tween-20 (PBST, manufacturer VWR). The suspension is pumped through the channel with a flow rate of 10 µl/min and the dwell time is set to 0.4 ms.

The fluorescence signal is recorded and single events above a threshold are evaluated. By creating a histogram of the signal intensities of the events, the conjugation populations are be distinguished. We determine the mean fluorescence signals by fitting Gaussian curves to the histogram. A calibration curve is defined by fitting a straight line to a plot of the mean fluorescence signals against the MESF values. The definition of the decision limit CC_α and the detection limit CC_β are derived from the German standard DIN 32645[12]. The decision limit is the level of MESF per particle, which generates a signal intensity only reached by the fraction α of measurements taken from a blank sample. α is the allowed type I error and chosen to be 1/600,000. At the given dwell time, this is equal to 0.25 false positive events per minute

$$CC_\alpha = \frac{\sigma}{b} \cdot t_{f;\alpha} \sqrt{\frac{1}{m} + \frac{1}{n}} \,. \tag{1}$$

Here, σ denotes the standard deviation, *b* the slope of the calibration curve, $t_{f;\alpha}$ the quantile of the t-distribution and *m*, *n* are the number of measurements per sample, the number of calibration samples used, respectively. The standard deviation of the signal intensities of each conjugation population can be described by $\sigma(x) = d \cdot b \cdot x$ where *x* is the conjugation level and *d* the determined proportionality factor. The detection limit is calculated by

$$CC_{\beta} = \frac{CC_{\alpha}}{1 - d \cdot t_{f;\beta} \cdot \sqrt{\frac{1}{m} + \frac{1}{n}}}. \qquad (2)$$

2.3 Setup for channel geometries with widths of 150 µm and 400 µm

For channel widths larger than 20 µm, the setup has to be modified. We studied two single channel setups for channel width of 150 µm and 400 µm, the channel depths amounts to 150 µm. A cylindrical lens is inserted between the excitation filter and the dichroic beamsplitter to generate an elliptic focus. The laser source used is a pulsed laser diode emitting at a wavelength of 650 nm (LDH 650-b, PicoQuant).

A laser beam with a Gaussian diameter ($1/e^2$) of 2 mm is generated by a fiber collimator. A laser clean up filter transmitting wavelengths between 650 nm to 660 nm, a dichroic beamsplitter transmitting wavelengths >660 nm and an emission filter for fluorescence light between 670 nm and 750 nm are used. A pair of lenses consisting of a cylindrical lens and a spherical plano-convex lens forms an elliptic laser focus (long axis parallel to *y*-direction, cf. Fig. 1)for fluorophore excitation. The cylindrical lens is positioned between excitation filter and dichroic mirror. In this way the collected fluorescence light does not pass the cylindrical lens on the way to the detector.

The fluorescence light excited in the laser focus and collected by the spherical lens is transmitted by the dichroic mirror. A slit is positioned in a confocal setup between the dichroic mirror and a single photon avalanche diode (SPAD) assembly (SPCM-AQR-13, Excelitas). The lenses used in the confocal setup are chosen to match the width of the slit with the short axis of the excitation focus (along the *x*-direction) and the desired measurement volume widths with the active detection area diameter of the SPAD, respectively.

For a 150 µm wide measurement volume a cylindrical lens with the focal length of 100 mm and a focusing lens with a focal length of 10 mm are used and for a 400 µm wide measurement volume a lens pair consisting of a cylindrical lens with a focal length of 75 mm and a focusing lens with a focal length of 25 mm.

We use beads with different amounts of the fluorophore FlashRed (Flash Red intensity standard, Bangs Laboratories) inside to characterize the sensors. Since an absolute quantification of the amount of fluorophore within the bead populations is not available, the amount of fluorophores is referenced to the population with maximum amount given in per-cent. For scanning the measurement volume one of maximal filled particles is immobilized on a glass slide, the further proceeding is as described in section 2.2. A signal-to-noise ratio is calculated determining the mean fluorescence signal of the 100% fraction divided by the standard deviation of the signal measured in the same configuration with a particle free solution of PBST.

3. RESULTS AND DISCUSSION

3.1 Measurement Volume

Using one of the two identical channels the measurement volume is determined. A 2D image of the relative sensitivity in the focal plane of the focusing lens is shown in Fig. 2. The measurement volume is slightly oval and the line plots in Fig. 3 reveal the widths of 29 µm and 33 µm in *x*- and *y*-direction. Taking the diameter of the measurement particles into account with 8 µm, the widths of the measurement volume are estimated to (21±1) µm and (25±1) µm in *x*- and in *y*-direction. The two channels of the setup show similar results. For simplification we show only the experimental data of one channel in detail.

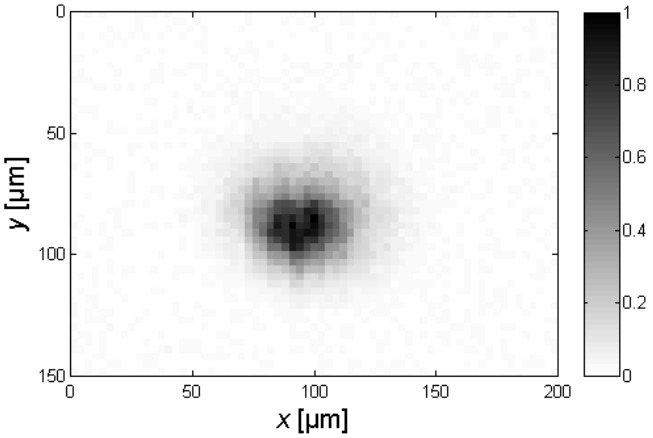

Fig. 2. 2D image of the relative sensitivity in the focal plane. The resolution of the scan amounts to 3 µm in the *x*- and *y*-direction.

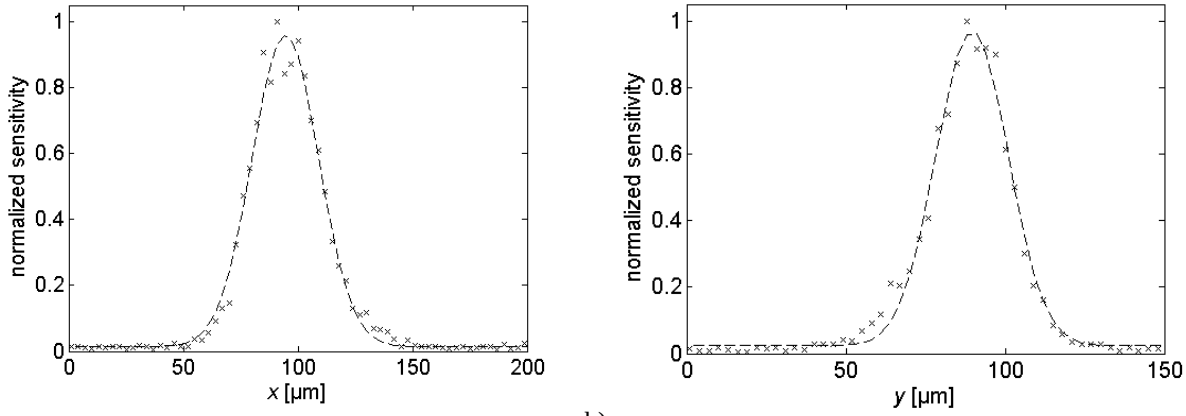

a) b)

Fig. 3. Line plots of relative sensitivity normalized to the maximum encountered fluorescence signal in the 2D scan. In a) a cut through the maximum in the *x*-direction is plotted and in b) a cut in the *y*-direction.

The sensitivity of the axial direction is analyzed by comparing the normalized maximum signal intensities at different *z*-positions. The data is plotted in Fig. 4 and indicates only a variation of less than 10 % within 150 µm around the focal plane, the channel depth used for determining the detection limit.

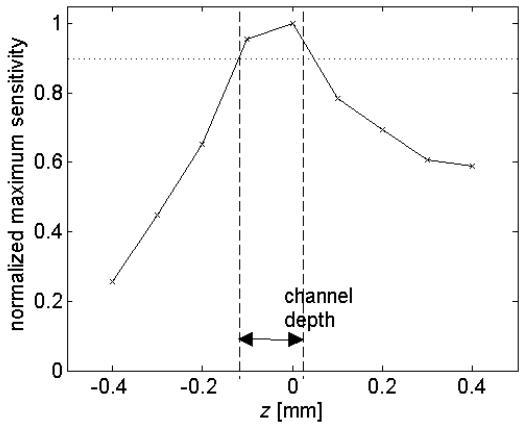

Fig. 4. The normalized maximum fluorescence signal as a function of the axial displacement *z*.

3.2 Detection Limit

A solution of particles with different fluorophore conjugation levels are measured in a microchannel. An excerpt of the experimental data is shown in Fig. 5. Particles passing the measurement volume cause signal peaks with different heights. The variations in height are due to different conjugation levels of the beads, the distribution of conjugation strength within one fraction and the nonuniform sensitivity within the measurement volume.

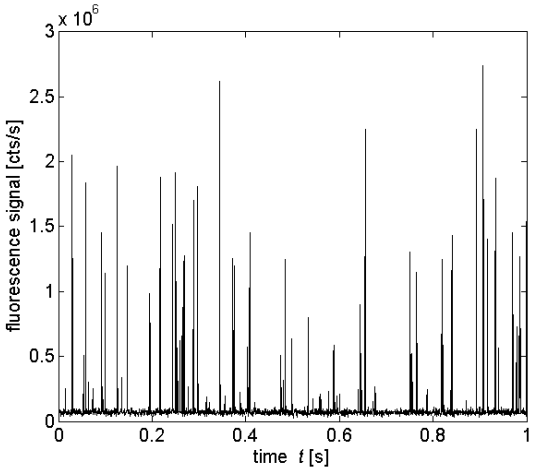

Fig. 5. Fluorescence signal with a dwell time of 0.4 ms and a flow rate of 10 µl/min. Shown is the first second of 120 seconds in total.

Figure 6 shows the heights of the peaks as a histogram revealing three populations of different conjugation levels. The mean value of each population is determined by fitting Gaussian curves to the respective distributions. The mean signal levels and the related MESF values are given in Fig. 6 and show a linear relation with a slope of (36 ± 1) cts/(s MESF), further used as slope for the calibration curve.

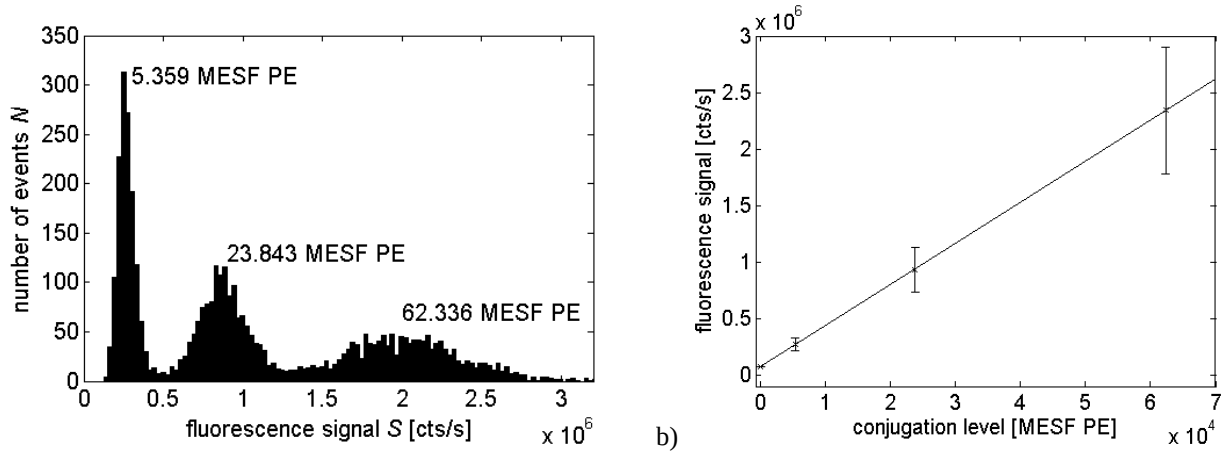

Fig. 6. Fluorescence signal distribution. a) The histogram shows the cumulated events for given fluorescence signal strengths. The three levels of PE conjugation are clearly distinguishable. b) The mean fluorescence signal intensities as function of the conjugation level and a reference measurement without particles. The error bars show the standard deviation and the solid line is a linear regression line with $R^2 = 1 - 1.7 \cdot 10^{-5}$.

By using the relations (1) and (2) the decision limit is determined to (1789 ± 93) MESF PE and the detection limit to (2851 ± 149) MESF PE. The second channel shows slightly higher decision limit of (1821 ± 94) MESF PE and detection limit of (3550 ± 183) MESF PE.

3.3 Measurement volume and SNR of wide channel setup

Due to the cylindrical lenses used in this setup elliptic foci are generated. The measurement volumes in the configuration for 150 µm wide channels and 400 µm wide channels are depicted in Fig. 7. The FWHM in *y*-direction is determined to be (145 ± 5) µm and (400 ± 25) µm.

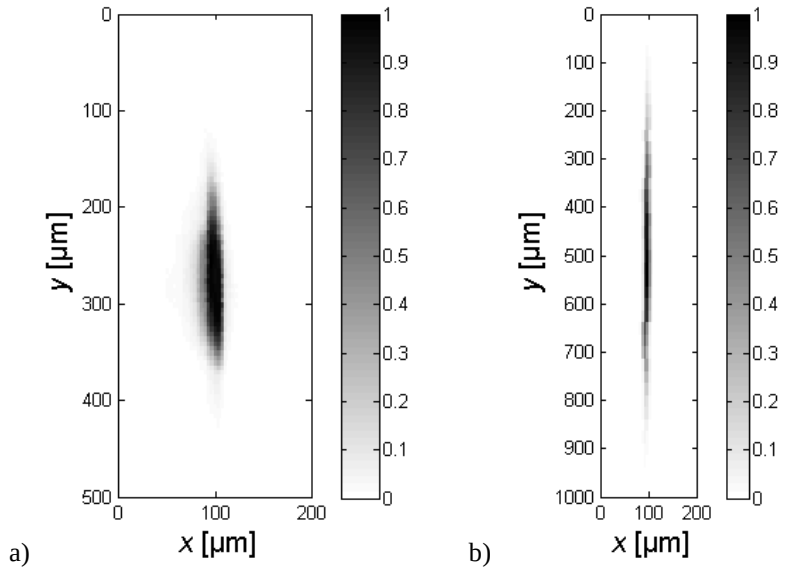

Fig. 7. 2D image of the relative sensitivity in the focal plane of the elliptic sensor. a) Measurement volume with FWHM of 145 µm in *y*-direction. b) Measurement volume with FWHM of 400 µm.

We use the fraction with the maximum amount fluorophore of the Flash Red intensity standard particles to determine a SNR of 1430 : 1 for the 150 µm setup at a flow rate of 20 µl/min and a SNR of 673 : 1 for the 400 µm setup at a flow rate of 10 µl/min.

4. CONCLUSIONS

Using a parallelized sensor we achieved a decision limit of 2009 MESF PE with a measurement volume diameter of 21 µm to 25 µm at a flow rate of 10 µl/min in a channel cross section of 20 µm width and 150 µm depth.

Another setup with two configurations was presented, whose measurement volumes could cover channels up to 150 µm and 400 µm wide. Signal-to-noise ratios of 1430 : 1 or 670 : 1 are demonstrated at flow rates up to 20 µl/min.

We demonstrated a highly versatile concept enabling parallelizing fluorescence sensors. The extension to 16 parallel sensors with measurement positions distributed in an area of 18 mm x 18 mm can be easily achieved. In a further expansion stage using all 64 anodes of the photomultiplier, we are able to implement 64 independent parallel fluorescence sensors.

With these concepts it is possible to increase the throughput of µTAS by using parallelized channel configurations, adding up the flow rates, and using higher flow rates with wide channel cross-sections, keeping the dwell time up and shear stress down because of smaller flow velocities and flow velocity gradients.

REFERENCES

[1] J. El-Ali, P. K. Sorger, and K. F. Jensen, "Cells on chips," Nature 442 (7101), 403–411 (2006).

[2] C. Yi, C.-W. Li, S. Ji, and M. Yang, "Microfluidics technology for manipulation and analysis of biological cells," Analytica Chimica Acta 560 (1-2), 1–23 (2006).

[3] B. F. Brehm-Stecher and E. A. Johnson, "Single-Cell Microbiology: Tools, Technologies, and Applications," Microbiology and Molecular Biology Reviews 68 (3), 538–559 (2004).

[4] G. Ryu, J. Huang, O. Hofmann, C. A. Walshe, J. Y. Y. Sze, G. D. McClean, A. Mosley, S. J. Rattle, J. C. deMello, A. J. deMello, and D. D. C. Bradley, "Highly sensitive fluorescence detection system for microfluidic lab-on-a-chip," Lab Chip 11 (9), 1664 (2011).

[5] C. M. Puleo, H. C. Yeh, K. J. Liu, and T. H. Wang, "Coupling confocal fluorescence detection and recirculating microfluidic control for single particle analysis in discrete nanoliter volumes," Lab Chip 8 (5), 822 (2008).

[6] C.-Y. Zhang, H.-C. Yeh, M. T. Kuroki, and T.-H. Wang, "Single-quantum-dot-based DNA nanosensor," Nat Mater 4 (11), 826–831 (2005).

[7] A. J. de Mello and J. B. Edel, "Hydrodynamic focusing in microstructures: Improved detection efficiencies in subfemtoliter probe volumes," J. Appl. Phys. 101 (8), 84903 (2007).

[8] G. Ryu, J. Huang, O. Hofmann, C. A. Walshe, J. Y. Y. Sze, G. D. McClean, A. Mosley, S. J. Rattle, J. C. deMello, A. J. deMello, and D. D. C. Bradley, "Highly sensitive fluorescence detection system for microfluidic lab-on-a-chip," Lab Chip 11 (9), 1664 (2011).

[9] B. K. McKenna, A. A. Selim, F. Richard Bringhurst, and D. J. Ehrlich, "384-channel parallel microfluidic cytometer for rare-cell screening," Lab Chip 9 (2), 305–310 (2009).

[10] X. Yan, W. K. Grace, T. M. Yoshida, R. C. Habbersett, N. Velappan, J. H. Jett, R. A. Keller, and B. L. Marrone, "Characteristics of different nucleic acid staining dyes for DNA fragment sizing by flow cytometry," Anal. Chem. 71 (24), 5470–5480 (1999).

[11] A. Schwartz, L. Wang, E. Early, A. Gaigalas, Y. Z. Zhang, G. E. Marti, and R. F. Vogt, "Quantitating fluorescence intensity from fluorophore: The definition of MESF assignment," J RES NATL INST STAN 107, 83–91 (2002).

[12] German standard DIN 32645, "Chemical analysis - Decision limit, detection limit and determination limit under repeatability conditions - Terms, methods, evaluation", (2008)